Journal for ImmunoTherapy of Cancer

Activated B cells suppress T-cell function through metabolic competition

Nobuhiko Imahashi,[1,2] Rafet Basar,[1] Yuefan Huang,[3] Fang Wang,[3] Natalia Baran,[4] Pinaki Prosad Banerjee,[1] Junjun Lu,[1] Ana Karen Nunez Cortes,[1] Nadima Uprety,[1] Emily Ensley,[1] Luis Muniz-Feliciano,[1] Tamara J Laskowski,[1] Judy S Moyes,[1] May Daher,[1] Mayela Mendt,[1] Lucila N Kerbauy,[1,5,6] Mayra Shanley,[1] Li Li,[1] Francesca Lorraine Wei Inng Lim,[1] Hila Shaim,[1] Ye Li ,[1] Marina Konopleva,[4] Michael Green,[7,8] Jennifer Wargo,[8,9] Elizabeth J Shpall,[1] Ken Chen,[3] Katayoun Rezvani [1]

To cite: Imahashi N, Basar R, Huang Y, *et al*. Activated B cells suppress T-cell function through metabolic competition. *Journal for ImmunoTherapy of Cancer* 2022;**10**:e005644. doi:10.1136/jitc-2022-005644

► Additional supplemental material is published online only. To view, please visit the journal online (http://dx.doi.org/10.1136/jitc-2022-005644).

Accepted 05 November 2022

For numbered affiliations see end of article.

Correspondence to
Dr Katayoun Rezvani;
krezvani@mdanderson.org

ABSTRACT

Background B cells play a pivotal role in regulating the immune response. The induction of B cell-mediated immunosuppressive function requires B cell activating signals. However, the mechanisms by which activated B cells mediate T-cell suppression are not fully understood.

Methods We investigated the potential contribution of metabolic activity of activated B cells to T-cell suppression by performing in vitro experiments and by analyzing clinical samples using mass cytometry and single-cell RNA sequencing.

Results Here we show that following activation, B cells acquire an immunoregulatory phenotype and promote T-cell suppression by metabolic competition. Activated B cells induced hypoxia in T cells in a cell–cell contact dependent manner by consuming more oxygen via an increase in their oxidative phosphorylation (OXPHOS). Moreover, activated B cells deprived T cells of glucose and produced lactic acid through their high glycolytic activity. Activated B cells thus inhibited the mammalian target of rapamycin pathway in T cells, resulting in suppression of T-cell cytokine production and proliferation. Finally, we confirmed the presence of tumor-associated B cells with high glycolytic and OXPHOS activities in patients with melanoma, associated with poor response to immune checkpoint blockade therapy.

Conclusions We have revealed for the first time the immunomodulatory effects of the metabolic activity of activated B cells and their possible role in suppressing antitumor T-cell responses. These findings add novel insights into immunometabolism and have important implications for cancer immunotherapy.

WHAT IS ALREADY KNOWN ON THIS TOPIC

⇒ Regulatory B cells are known to contribute to T-cell dysfunction but the metabolic immunomodulatory effect of activated B cells to T cell-mediated antitumor responses is not well understood.

WHAT THIS STUDY ADDS

⇒ Activated B cells suppress T-cell function by causing glucose and oxygen deficiency and leading to lactic acid poisoning. Tumor-associated B cells with high metabolic activities in patients with melanoma are associated with poor response to immune checkpoint blockade therapy.

HOW THIS STUDY MIGHT AFFECT RESEARCH, PRACTICE OR POLICY

⇒ Our findings provide new insight into the immunometabolism role of activated B cells in antitumor T-cell responses and their potential implications for cancer immunotherapy.

INTRODUCTION

B cells promote immune responses by producing antibodies and presenting antigens to T cells. Previous studies have reported that a subset of human B cells termed regulatory B cells (Bregs) are capable of inhibiting T-cell function.[1 2] While previous studies elucidating the mechanism of T-cell suppression by Bregs focused on classical mediators of immunosuppression such as interleukin (IL)-10 and transforming growth factor-β,[1–3] others have shown that the suppressive function of Bregs was at least partially dependent on signaling through CD40, CD80, and CD86.[1 2] Moreover, healthy donor-derived peripheral blood B cells acquire immunosuppressive properties on activation through the B cell receptor, CD40, or toll-like receptor (TLR), in the presence or absence of cytokines, whereas those from patients with autoimmune disease were unable to acquire such properties.[3–6] Similarly, induction of B cells with T cell-suppressive function in response to IL-21 and TLR ligands in human tumor microenvironment has been reported.[7 8] Finally, adoptive transfer of B cells stimulated through CD40 or TLR ex vivo ameliorated autoimmune disease in mice.[9 10] Collectively, these findings suggest a pivotal role for B cells in regulating the immune response,

and indicate that B cell activating signals are required for the induction of B cell-mediated immunosuppressive function.

On activation, B cells undergo metabolic reprogramming, enhancing their glycolytic and oxidative phosphorylation (OXPHOS) activities.[11] Recent studies in cancer have unveiled the immunomodulatory effects of cellular metabolism, with highly glycolytic tumors shown to disrupt immune surveillance by T cells through glucose deprivation and lactic acid production, resulting in tumor progression.[12–14] In addition, although it has not been explored, elevated OXPHOS activity of cells may have immunomodulatory effects as cells may induce hypoxia in adjacent T cells by consuming oxygen via OXPHOS, leading to T-cell dysfunction.[15] These findings raise the hypothesis that activated B cells suppress T-cell function by causing glucose and oxygen deficiency and leading to lactic acid poisoning through their high glycolytic and OXPHOS activity. Here we demonstrate that activated B cells upregulate glycolysis and OXPHOS and this metabolic change leads to immunomodulatory effects that may play an important role in inhibition of T cell-mediated antitumor responses.

MATERIALS AND METHODS

Cell isolation

Human $CD4^+$ T cells, $CD8^+$ T cells and $CD19^+$ B cells were isolated using magnetic microbeads (Miltenyi Biotec). B cells were sorted into naïve, transitional, IgM memory, and switched memory B cells by FACSAria II (Becton Dickinson) as previously reported.[1] Details of cell isolation methods are provided in the online supplemental methods.

B cell culture

Iscove's Modified Dulbecco's Medium containing 10% fetal bovine serum, 2 mM L-glutamine, 100 U/mL penicillin and 100 µg/mL streptomycin (all from HyClone) was used for B cell culture. To generate activated B cells, freshly isolated $CD19^+$ B cells were stimulated with CpG ODN 2006 (CpG) (3 µg/mL, Hycult Biotech), anti-IgM/IgG goat-α-human F(ab′)2 (anti-BCR) (10 µg/mL, Jackson ImmunoResearch Laboratories), and IL-2 (100 U/mL, PeproTech) for 60 hours at 37°C in a humidified atmosphere containing 21% O_2 and 5% CO_2. To inhibit glycolysis of B cells, B cells were treated with lactate dehydrogenase (LDH) inhibitor GSK 2837808A (50 µM, Tocris) for the last 24 hours of the stimulation. In some experiments, freshly isolated $CD19^+$ B cells were stimulated with CD40 ligand (CD40L) (100 ng/mL, AdipoGen) and IL-4 (10 ng/mL, PeproTech) for 60 hours. As B cells undergo apoptosis rapidly without cytokines,[16] B cells cultured in the presence of IL-4 (10 ng/mL, PeproTech) were used as a control (resting B cells).

B cell and T-cell co-culture

$CD4^+$ or $CD8^+$ T cells and B cells were co-cultured in 96-well flat-bottom plates at 1:1 ratio unless otherwise specified. To block direct contact between B and T cells, 96-well transwell chambers (0.4 µm pore size, Millipore) were used. In some experiments, the following reagents were added to the culture; anti-CD80 Ab (37711; 10 µg/mL; R&D Systems), anti-CD86 Ab (IT2.2; 10 µg/mL; BioLegend), anti-PD-L1 Ab (MIH1; 10 µg/mL; eBioscience), IL-2 (500 U/mL, PeproTech), and lactic acid (Santa Cruz Biotechnology). Isotype control Ab was used at the same concentration as the specific Ab. Details of co-culture assay are provided in the online supplemental methods.

Flow cytometry

Flow cytometry was used to assess the expression of intracellular antigens, cell proliferation, phosphorylation of proteins, and intracellular hypoxia. Details of these assays are provided in the online supplemental methods.

Metabolic flux analysis

$CD4^+$ or $CD8^+$ T cells and activated B cells were cultured for 24 hours (as described in the culture experiment section), and then separated by magnetic beads (as described in the cell isolation section). Purified $CD4^+$ T cells and activated B cells were then subjected to the Seahorse Mito Stress Test (Agilent Technologies), and the oxygen consumption rate (OCR) and extracellular acidification rate were measured by Seahorse XFe96 analyzer according to the manufacturer's instructions. Briefly, cells were washed twice with phosphate-buffered saline and finally resuspended in Seahorse Basal Medium (pH 7.4), supplemented with 1 mM pyruvate, 2 mM glutamine and 10 mM glucose. Cells were suspended (175 µL) at the density of 2–2.5 million/mL and were plated in a 96-well plate, previously precoated with Cell-Tak in 4–5 replicates, followed by gentle centrifugation at 1000 g without break to allow the cells to attach to the bottom. Three measurements of OCR were obtained at baseline, and following the sequential addition of oligomycin (1.5 µM), carbonyl cyanide-4 (trifluoromethoxy) phenylhydrazone (FCCP) (1.0 µM) and rotenone and antimycin A (R/A) (0.5 µM). All measurements were normalized to viable cell numbers and analyzed in a Mito Stress Test Generator (Agilent Technologies).

Measurement of glucose and L-lactate concentration

Supernatants from co-culture experiments were collected after 48 hours of co-culture. Alternatively, T or B cells were resuspended in culture medium at 2×10^6 cells/mL, incubated for 6 hours, and then supernatants were collected. Glucose and L-lactate concentration in the supernatant were measured by the Glucose and L-Lactate Assay Kits (Abcam, Cambridge, Massachusetts, USA), respectively, according to the manufacturers' instructions.

Patient samples

Peripheral blood samples used in this study were collected from patients with melanoma treated on a clinical trial of neoadjuvant immune checkpoint blockade (ICB) at MD Anderson Cancer Center (NCT02519322). Responders were defined as having complete or partial response by response evaluation criteria in solid tumours (RECIST) V.1.1 criteria and non-responders as having less than a partial response.

Mass cytometry

In-depth characterization of B cells stimulated in vitro and those from patients with melanoma who received ICB therapy was performed using metal-tagged antibodies as previously described and shown in online supplemental methods and online supplemental table 1.[17]

Bulk RNA sequencing

RNA was extracted and purified from B cells and T cells using the RNeasy Plus Mini Kit (Qiagen) and sent for RNA sequencing at MD Anderson's core facility, where quality control, library construction and sequencing were performed. Details of bulk RNA sequencing data analysis are provided in the online supplemental methods.

Single-cell RNA sequencing

To characterize B cells in human tumor tissues, we retrieved public single-cell RNA sequencing (scRNA-seq) data from the NCBI Gene Expression Omnibus database accession code GSE120221, GSE72056, GSE103322, and from ArrayExpress under accessions E-MTAB-6149. scRNA-seq data for normal lung B cells were downloaded from the Human Lung Cell Atlas (https://hlca.ds.czbiohub.org/). Details of scRNA-seq data analysis are provided in the online supplemental methods.

Statistical analyses

Unless otherwise indicated, data are expressed as means±SD. Two-group comparisons were performed with paired or unpaired Student's t-test. Multiple groups were compared by analysis of variance with Bonferroni's post hoc test. Differences were considered significant when $p<0.05$. GraphPad Prism V.9.0 was used for statistical analysis.

RESULTS

B cells activated in vitro suppress the mammalian target of rapamycin pathway in T cells

We first validated the immunosuppressive properties of B cells activated in vitro, which has been reported previously.[3 6 7] Human peripheral blood B cells stimulated with CpG, anti-IgG/IgM, and IL-2 (activated B cells), but not resting B cells, significantly suppressed interferon-γ, tumor necrosis factor-α, and IL-2 production and proliferation of $CD4^+$ and $CD8^+$ T cells following co-culture (figure 1A,B; online supplemental figure S1). In contrast, the absolute numbers of activated B cells after culture were higher when they were co-cultured with T cells in the presence of anti-CD3/CD28 beads than when they were cultured alone (data not shown), suggesting that the proliferation of activated B cells was supported by T cells. When the suppressive properties of different B cell subsets were analyzed, we found that all B cell subsets except transitional B cells, which comprises less than 10% of peripheral B cells, acquired immunosuppressive properties on activation (online supplemental figure S2). We asked whether activated B cells mediated their immunosuppressive effects by altering the properties of $CD4^+$ T cells. Activated B cells did not induce upregulation of markers associated with T regulatory (Treg) cells or exhaustion in $CD4^+$ T cells following co-culture (data not shown). A significant proportion of $CD4^+$ T cells precultured with activated B cells were able to produce effector cytokines once they separated from activated B cells (figure 1C), indicating that activated B cells do not alter the properties of $CD4^+$ T cells. Rather, suppression of $CD4^+$ T cells by activated B cells is a reversible process.

To explore the hypothesis that activated B cells suppress T-cell function by causing glucose and oxygen deficiency through their high glycolytic and OXPHOS activity, we first asked whether T cells co-cultured with activated B cells are metabolically restricted. To this end, we assessed mammalian target of rapamycin (mTOR) activity in T cells since mTOR plays a central role in regulating T-cell effector function, and both glucose deficiency and hypoxia lead to mTOR pathway suppression.[15] Indeed, we observed a decrease in phosphorylation of mTOR and ribosomal protein S6 (S6), a downstream target of mTOR, in $CD4^+$ and $CD8^+$ T cells stimulated in the presence of activated B cells compared with those stimulated alone (figure 1D,E, online supplemental figure S1C). Resting B cells did not inhibit the mTOR pathway in $CD4^+$ T cells (online supplemental figure S3). We also examined phosphorylation of other proteins involved in T-cell receptor signaling including ZAP70, p38, ERK, and JNK, but none of them were affected by activated B cells (online supplemental figure S4). These results suggest that activated B cells suppress T-cell function by inhibiting the activity of the mTOR pathway. Although activated B cells suppressed both $CD4^+$ and $CD8^+$ T cells, we focused the remainder of our studies on $CD4^+$ T cells.

Activated B cells induce hypoxia in $CD4^+$ T cells by consuming more oxygen via OXPHOS

To determine if activated B cells inhibit the mTOR pathway by inducing hypoxia in $CD4^+$ T cells, we compared the mitochondrial OCR between $CD4^+$ T cells and activated B cells isolated after 24 hours co-culture. Purified activated B cells had a significantly higher mitochondrial OCR when compared with purified $CD4^+$ T cells (figure 2A). Moreover, activated B cells isolated after co-culture with anti-CD3/CD28 bead-activated $CD4^+$ T cells displayed higher mitochondrial OCR than those cultured alone or those cultured with $CD4^+$ T cells in the absence of anti-CD3/CD28 beads (unstimulated T cells) (figure 2B). A similar phenomenon was observed between activated B

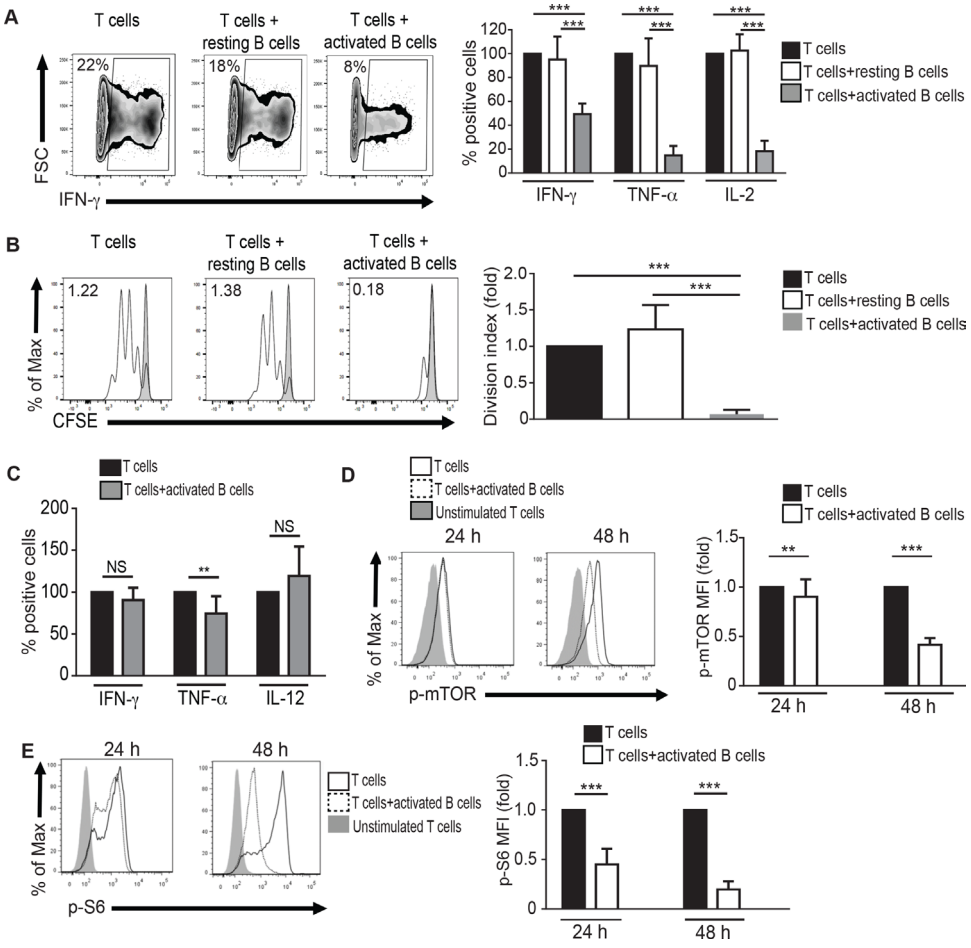

Figure 1 Activated B cells suppress the mTOR pathway in CD4$^+$ T cells. (A) IFN-γ, TNF-α, and IL-2 production by CD4$^+$ T cells that were cultured alone, with resting B cells, or with activated B cells in the presence of anti-CD3/CD28 beads. PMA/ionomycin and BFA were added for the last 4 hours of a 48 hours culture period. Representative flow plots (left panel) and summary of frequencies of cytokine-positive cells among CD4$^+$ T cells, presented relative to CD4$^+$ T cells stimulated alone, set as 100% (right panel); n=11. (B) Representative flow plots of CFSE dilution assay of CD4$^+$ T cells cultured for 72 hours as described in (A) (left panel) and summary of division index of CD4$^+$ T cells, presented relative to CD4$^+$ T cells stimulated alone, set as 1 (right panel). Numbers in the plots indicate division index. n=11. (C) IFN-γ, TNF-α, and IL-2 production by CD4$^+$ T cells which were precultured alone or with activated B cells in the presence of anti-CD3/CD28 beads for 2–4 days, purified and rested for 2–3 days, and then restimulated with anti-CD3/CD28 beads in the presence of BFA for 4 hours. Summary of frequencies of cytokine-positive cells among CD4$^+$ T cells, presented relative to those of CD4$^+$ T cells precultured alone, set as 100% (right). n=7. (D, E) Representative histograms showing the phosphorylation of mTOR (D) and S6 (E) in CD4$^+$ T cells cultured alone or stimulated with anti-CD3/CD28 beads in the absence or presence of activated B cells for 24 or 48 hours. Representative flow histograms (left) and summary of median fluorescent intensity (MFI), presented relative to CD4$^+$ T cells stimulated alone, set as 1.0 (right). n=18. Statistical analysis by repeated measures two-way (A, C, D, E) or one-way (B) analysis of variance with Bonferroni's correction for multiple comparisons. CFSE, carboxyfluorescein succinimidyl ester; FSC, forward scatter; IFN, interferon; IL, interleukin; mTOR, mammalian target of rapamycin; NS, not significant; p-mTOR, phospho-mTOR; TNF, tumor necrosis factor. *p≤0.05, **p≤0.01, ***p≤0.001.

cells and CD8$^+$ T cells (online supplemental figure S5). Taken together, these results indicate that activated B cells have a higher mitochondrial OCR compared with CD4$^+$ T cells.

Next, we asked whether activated B cells can induce intracellular hypoxia in CD4$^+$ T cells by consuming more oxygen via OXPHOS. We found that anti-CD3/CD28 bead-activated CD4$^+$ T co-cultured with activated B cells showed significant staining for two well-described markers of intracellular hypoxia, pimonidazole and MAR (figure 2C; online supplemental figures S6 and S7).[18] In contrast, pimonidazole and MAR were not expressed in bead-activated CD4$^+$ T cells cultured alone or with resting B cells (figure 2C; online supplemental figures S6 and S7). To further confirm the induction of hypoxia in activated CD4$^+$ T cells co-cultured with activated B cells, we examined the expression of hypoxia-inducible factor 1-α (HIF-1α), a molecule that is rapidly degraded by the ubiquitin-proteasome system under normoxia, but stabilized under hypoxia.[19] We found that bead-activated CD4$^+$ T cells co-cultured with activated B cells expressed higher levels of HIF-1α and hypoxia-related genes compared

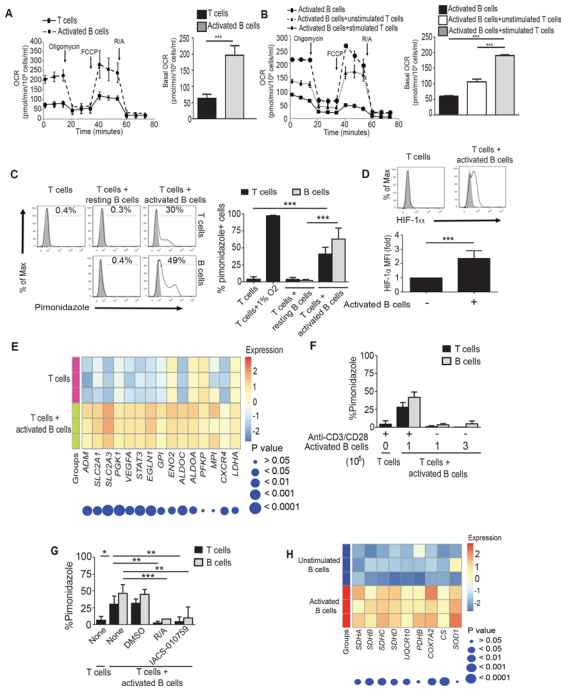

Figure 2 Activated B cells induce hypoxia in CD4$^+$ T cells by consuming oxygen via OXPHOS. (A) Oxygen consumption rates (OCR) of CD4$^+$ T cells and activated B cells which were co-cultured in the presence of anti-CD3/CD28 beads for 24 hours, and then separated by magnetic beads. OCR was determined by Seahorse assay (left panel). Data are representative of three independent experiments, performed in triplicate, with n=3 individual samples (right panel). (B) OCR of purified activated B cells that were precultured alone, or co-cultured with CD4$^+$ T cells in the absence or presence of anti-CD3/CD28 beads for 24 hours. Activated B cells were then purified by magnetic beads and their OCR was determined by Seahorse assay (left). Data are representative of two independent experiments, performed in triplicate, with n=3 individual samples (right). (C) Pimonidazole staining of CD4$^+$ T cells (upper row) and B cells (lower row) cultured for 48 hours in the presence of anti-CD3/CD28 beads. Representative flow histograms (left) and summary of frequencies of pimonidazole$^+$ cells among CD4$^+$ T and CD19$^+$ B cells (right). n=11. The gray histograms indicate negative control. Data from T cells stimulated under hypoxia (1% O_2) is shown as a positive control (n=5). (D) HIF-1a expression in CD4$^+$ T cells stimulated with anti-CD3/CD28 beads alone or in the presence of activated B cells for 24 hours. Representative flow histograms (top panel) and summary of HIF-1a MFI in CD4$^+$ T cells, presented relative to CD4$^+$ T cells stimulated alone, set as 1 (bottom panel). The gray histograms indicate isotype control. n=7. (E) Comparative heat map of RNA sequencing data showing the expression of hypoxia-related genes between CD4$^+$ T cells stimulated alone or those stimulated in the presence of activated B cells. Each row represents T cells from a different donor (n=3). Color scale ranges from blue (low expression) to red (high expression). The FDR-adjusted p values for each gene are shown under the heat map. (F) CD4$^+$ T cells (1×10^5) were cultured alone, with activated B cells (1×10^5) in the presence of anti-CD3/CD28 beads, or with activated B cells ($1–3\times10^5$) in the absence of anti-CD3/CD28 beads for 48 hours. Summary of frequencies of pimonidazole$^+$ cells among CD4$^+$ T and CD19$^+$ B cells is shown. n=5. (G) Pimonidazole staining of CD4$^+$ T and activated B cells co-cultured for 48 hours under anti-CD3/CD28 bead stimulation. DMSO (solvent control), a combination of rotenone and antimycin A (R/A) (0.5 mM), or IACS-010759 (45 nM) were added for the last 5 hours of the co-culture. n=7. (H) Comparative heat map of RNA sequencing data showing the expression of OXPHOS-related genes between unstimulated B cells and activated B cells. Each row of heatmap represents B cells from a different donor (n=3) and each column represents the expression of a certain marker for each annotation. Color scale ranges from blue (low expression) to red (high expression). The FDR-adjusted p value for each gene is shown under the heat map. Statistical analysis by ordinary one-way (B) or repeated measures one-way analysis of variance (C, G) with Bonferroni's corrections for multiple comparisons, unpaired t-test (A) or paired t-test (D). *p≤0.05, **p≤0.01, ***p≤0.001. DMSO, dimethyl sulfoxide; FDR, false discovery rate; HIF, hypoxia-inducible factor; MFI, median fluorescent intensity; OXPHOS, oxidative phosphorylation.

with CD4$^+$ T cells cultured alone both by flow cytometry and messenger RNA expression (figure 2D,E).[20 21] Collectively, all these results indicate that activated B cells induce intracellular hypoxia in co-cultured activated CD4$^+$ T cells. Importantly, when CD4$^+$ T cells were co-cultured with activated B cells in the absence of anti-CD3/CD28 bead activation, neither CD4$^+$ T cells nor activated B cells became hypoxic, even when higher numbers of activated B cells were added to the well (figure 2F), suggesting that the high mitochondrial OCR of activated B cells is supported by CD4$^+$ T-cell activation (figure 2B) and is required for induction of hypoxia in CD4$^+$ T cells. Together, these data support that induction of hypoxia in CD4$^+$ T cells by activated B cells is an active process that requires B–T-cell interaction and is not merely the effect of higher numbers of cells per well.

Cells consume oxygen either through OXPHOS or non-mitochondrial respiration. To confirm that induction of hypoxia in CD4$^+$ T cells by activated B cells is due to oxygen consumption associated with OXPHOS,

we added OXPHOS inhibitors (combination of R/A or IACS-010759[22] to the culture, and assessed intracellular hypoxia in T cells and B cells by pimonidazole staining. Both R/A and IACS-010759 significantly diminished the induction of hypoxia in co-cultured CD4+ T and activated B cells (figure 2G), confirming that the induction of hypoxia in CD4+ T cells by activated B cells is due to increased oxygen consumption associated with OXPHOS metabolism. Finally, we confirmed that activated B cells had higher expression of OXPHOS-related genes compared with unstimulated B cells (figure 2H), further confirming the higher mitochondrial OCR in activated B cells.[23]

Induction of hypoxia in CD4+ T cells by activated B cells requires cell–cell contact

To determine if activated B cells induced hypoxia in T cells by simply competing for oxygen in the media as shown for activated neutrophil-induced hypoxia in epithelial cells,[24] or if the process requires crosstalk and cell–cell contact, we performed transwell experiments, where CD4+ T cells were either in direct contact with, or separated from activated B cells by permeable inserts. The increase in pimonidazole staining observed in CD4+ T cells which were in direct contact with activated B cells was completely lost when CD4+ T cells were physically separated from activated B cells (figure 3A), while activated B cells continued to be positive for pimonidazole (figure 3A; the fifth gray bar from the left). The observation that activated B cells were hypoxic, while CD4+ T cells physically separated from activated B cells were not, suggests that activated B cells do not induce hypoxia in CD4+ T cells by causing global oxygen deficiency in the culture, but rather do so through physical contact. This view is supported by the finding that the degree of hypoxia was even greater in CD4+ T cells conjugated with two activated B cells than in those conjugated with one activated B cell as assessed by imaging flow cytometry (figure 3B). Taken together, these results indicate that activated B cells induce intracellular hypoxia in CD4+ T cells in a cell–cell contact dependent manner.

Activated B cells suppress the mTOR signaling pathway and effector function of CD4+ T cells through induction of hypoxia

Next, we asked whether hypoxia induced by activated B cells is involved in the suppression of the mTOR pathway

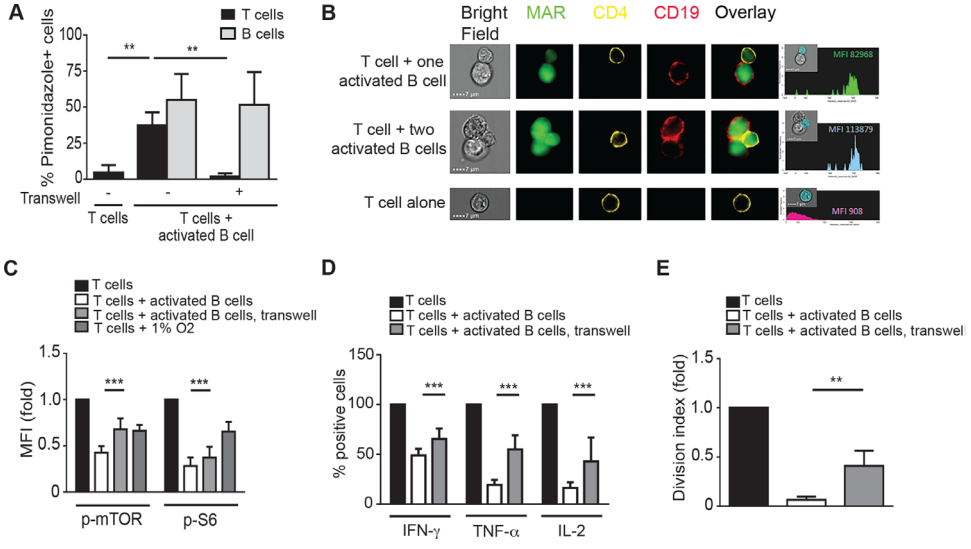

Figure 3 Hypoxia induction in CD4+ T cells by activated B cells is dependent on cell–cell contact and causes T-cell suppression. (A) CD4+ T cells were cultured alone, with activated B cells, or with activated B cells separated by transwell inserts in the presence of anti-CD3/CD28 beads for 48 hours. Bar graphs show the mean frequencies±SD of pimonidazole+ cells among CD4+ T (black bars) and CD19+ B cells (gray bars), n=6. (B) CD4+ T cells were cultured alone or with activated B cells in the presence of anti-CD3/CD28 beads for 36 hours, and then cells were subjected to imaging flow cytometry analysis. Representative images of cells are displayed in bright fields and expressions of MAR (green), CD4 (yellow) and CD19 (red); an overlay of all fluorescent channels is also shown. The last column shows the expression of MAR inside the mask (teal) of the CD4+ T cells in conjugate with one (top row) or two (middle row) activated B cells or CD4+ T cells stimulated alone (bottom row). Histograms show the MFI of MAR as defined by the mask for a given cell under consideration. Note the stronger MAR staining of CD4+ T cells conjugated with two activated B cells compared with those conjugated with one activated B cell. Data are a representative of two independent experiments, scale bar=7 mm. (C) Phosphorylation of mTOR and S6 in CD4+ T cells cultured alone, with activated B cells, or with activated B cells separated by transwell inserts in the presence of anti-CD3/CD28 beads for 48 hours, n=18. Data from T cells stimulated under hypoxia (1% O_2) are shown as a reference (n=5). (D, E) CFSE-labeled CD4+ T cells were cultured alone, with activated B cells, or with activated B cells separated by transwell inserts in the presence of anti-CD3/CD28 beads. Suppression of CD4+ T-cell IFN-γ, TNF-α, and IL-2 production (D) and proliferation (E) are shown as in figure 1A and B, respectively. n=7. Statistical analysis by repeated measures one-way (A, E) or two-way (C, D) analysis of variance with Bonferroni's correction for multiple comparisons. **p≤0.01, ***p≤0.001. CFSE, carboxyfluorescein succinimidyl ester; IFN, interferon; IL, interleukin; MFI, median fluorescent intensity; p-mTOR, phospho-mTOR; TNF, tumor necrosis factor.

in CD4+ T cells. When induction of hypoxia in CD4+ T cells was inhibited by physically separating CD4+ T cells from activated B cells, hypophosphorylation of mTOR and S6 was partially but significantly reversed (figure 3C), suggesting that activated B cells suppress the mTOR pathway in CD4+ T cells by inducing hypoxia. On the other hand, blockade of surface molecules employed by Bregs to suppress T cells such as CD80, CD86, and programmed death-ligand 1 (PD-L1) did not reverse the suppression of the mTOR pathway (online supplemental figure S8A,B).[2 25] In addition, although activated B cells highly expressed IL-2 receptor subunit alpha (IL-2Rα) (data not shown), which is responsible for IL-2 deprivation from T effector cells by Treg cells,[26] addition of exogenous IL-2 to the co-culture did not reverse the mTOR pathway suppression (online supplemental figure S8C,D). Thus, these molecules are unlikely to be involved in the CD4+ T-cell mTOR pathway suppression by activated B cells.

Finally, blockade of cell–cell contact by transwell separation partially reversed the suppression of CD4+ T-cell cytokine production and proliferation (figure 3D,E). Taken together, these results indicate that intracellular hypoxia induced by activated B cells results in suppression of the mTOR pathway and effector function of CD4+ T cells.

Activated B cells are able to inhibit the mTOR pathway in T cells through glycolytic activity

Partial reversal of CD4+ T-cell suppression by activated B cells in the transwell experiments (figure 3C–E) suggests that an additional mechanism by which activated B cells suppress CD4+ T cells exists. In this regard, it is noteworthy that activated B cells had higher expression of glycolysis-related genes in addition to OXPHOS-related genes than did unstimulated B cells, indicating their high glycolytic activity (figure 4A).[27] Glucose deficiency has been reported to suppress the mTOR pathway in CD4+ T cells.[28] In addition, similar to a recent study that showed an inhibitory effect of lactic acid, an end product of glycolysis, on the mTOR pathway in CD8+ T cells,[14] we found that lactic acid suppressed the mTOR pathway in CD4+ T cells (figure 4B,C). Thus, we hypothesized that activated B cells suppress the mTOR pathway in CD4+ T cells through glucose deprivation and lactic acid production.

To test this hypothesis, we assessed the glycolytic activity of activated B cells and CD4+ T cells by measuring their glucose consumption and lactate production. Anti-CD3/CD28 bead-activated CD4+ T cells were co-cultured with activated B cells for 24 hours. Cells were then subjected to magnetic separation as described in the Methods to obtain purified CD4+ T and activated B cells. The results showed higher glucose consumption and lactate production by activated B cells compared with CD4+ T cells (figure 4D,E). This was partly due to enhancement of glycolytic activity in activated B cells by CD4+ T cells, as demonstrated by higher glucose consumption and lactate production in activated B cells precultured with CD4+ T cells than when activated B cells were cultured alone (figure 4F,G). Finally, when activated CD4+ T cells were cultured in the presence of activated B cells, glucose levels were markedly reduced while lactate levels were increased in the culture media (figure 4H,I), supporting our hypothesis that activated B cells suppress the mTOR pathway in CD4+ T cells through glucose deprivation and lactic acid production. Indeed, CD4+ T-cell mTOR pathway suppression by activated B cells was partially reversed when glycolysis of activated B cells was inhibited by LDH inhibitor (figure 4J). Importantly, glucose and lactate levels were largely unchanged when anti-CD3/CD28 bead-activated CD4+ T and activated B cells were separated by transwell inserts (online supplemental figure S9), which makes it unlikely that change in the glucose and lactic acid concentration in the culture media played a major role in the reversal of CD4+ T-cell mTOR pathway suppression in the transwell experiments (figure 3C).

B cells with activated phenotype can be identified in human tumor tissues and are associated with poor response to ICB therapy

We next aimed to identify markers characteristic of activated B cells with immunosuppressive properties. We analyzed B cells stimulated with CD40L and IL-4 (reported to induce B cells that function as antigen-presenting cells rather than immunosuppressive cells),[29] versus activated B cells stimulated with CpG, anti-IgG/IgM, and IL-2 versus unstimulated B cells. We confirmed that B cells stimulated with CD40L and IL-4 did not inhibit T-cell function (online supplemental figure S10). Using viSNE, a t-distributed stochastic neighbor-embedding algorithm we found that, as expected, activated B cells had higher expression of most of the B cell activation markers compared with unstimulated B cells (figure 5A,B).[6 30–33] However, we found that while B cells simulated with CD40L and IL-4 upregulated some of the B cell activation markers compared with unstimulated B cells, four antigens CD39, CD80, PD-L1, and programmed cell death protein 1 (PD-1) were more specifically increased in CpG+anti-IgG/IgM+IL-2-activated B cells (figure 5B). Thus, these four markers may serve as markers to identify activated B cells with immunosuppressive function.

The tumor microenvironment is composed of various types of immune cells including B cells, which are termed tumor-associated B cells (TAB). Previous studies have shown antitumor T-cell inhibition by TAB.[34] To ask if TABs with immunosuppressive properties have a similar phenotype to activated B cells (B cells stimulated with CpG, anti-IgG/IgM, and IL-2 in vitro), we compared the phenotype of B cells from responders (n=6) to that from non-responders (n=6) among patients with melanoma who received ICB therapy. We did not observe a clear difference in peripheral blood B cell clusters between those two groups of patients (figure 5C). However, one B cell cluster (cluster #15 in figure 5C), which accounted for less than 5% of TABs in responders, showed a significant proportional increase in tumor tissues of non-responders (20%). Notably, this B cell cluster had higher expression of B cell activation markers, including CD39,

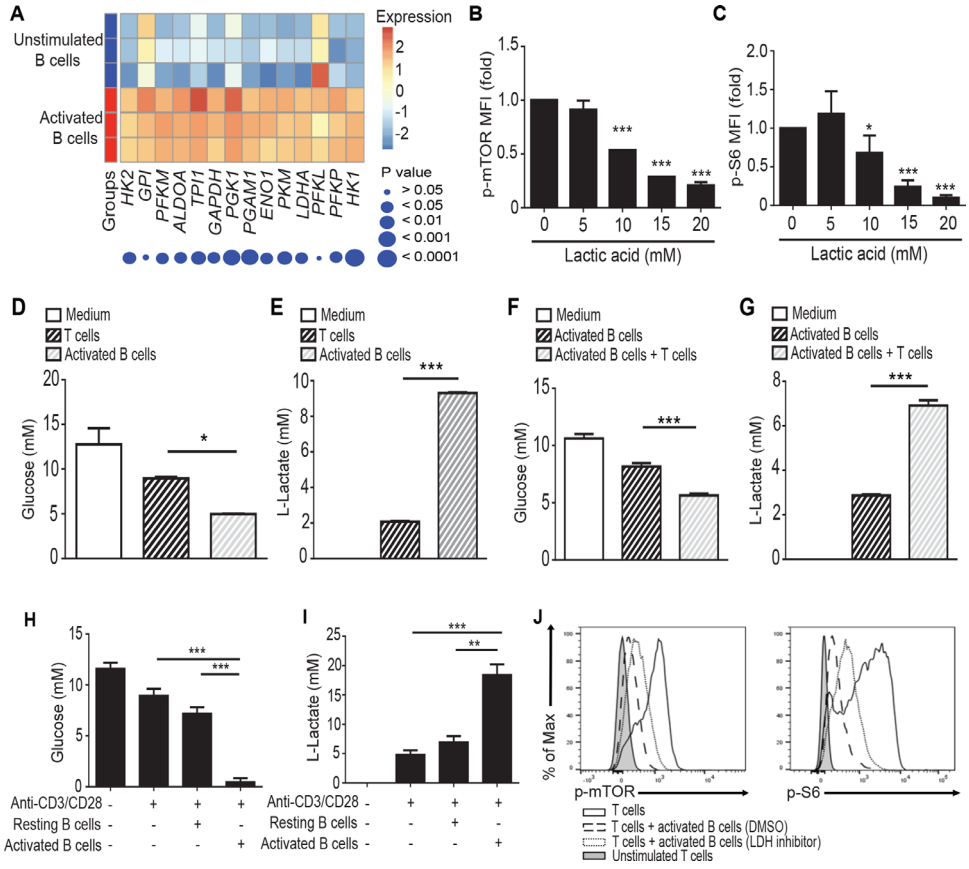

Figure 4 Activated B cells inhibit the mTOR pathway in CD4$^+$ T cells through their higher glycolytic activity. (A) Comparative heat map of RNA sequencing data showing the expression of glycolysis-related genes between unstimulated B cells and activated B cells. Each row of heatmap represents B cells from a different donor (n=3) and each column represents the expression of a certain marker for each annotation. Color scale ranges from blue (low expression) to red (high expression). The FDR-adjusted p values for each gene are shown under the heat map. (B, C) Bar graphs showing the phosphorylation of mTOR (B) and S6 (C) as assessed by phospho-specific flow cytometry in CD4$^+$ T cells which were stimulated with anti-CD3/CD28 beads in the absence or presence of lactic acid (5, 10, 15, 20 mM) for 48 hours. MFI is presented relative to CD4$^+$ T cells stimulated in the absence of lactic acid, set as 1.0. n=7. (D, E) Glucose consumption (D) and lactate production (E) by purified CD4$^+$ T cells and activated B cells which were precultured together in the presence of anti-CD3/CD28 beads for 24 hours, purified by magnetic beads, and then cultured alone in culture medium for an additional 6 hours. Data are representative of two independent experiments, performed in triplicate, with n=3 individual samples. (F, G) Glucose consumption (F) and lactate production (G) by activated B cells which were precultured alone or together with CD4$^+$ T cells in the presence of anti-CD3/CD28 beads for 24 hours, purified by magnetic beads, and then cultured alone in culture medium for an additional 6 hours. Data are representative of two independent experiments, performed in triplicate, with n=3 individual samples. (H, I) Glucose (H) and lactate (I) concentration in the supernatant of CD4$^+$ T cells cultured alone, with resting B cells, or with activated B cells in the presence of anti-CD3/CD28 beads for 48 hours. n=5. (J) Representative histograms showing the phosphorylation of mTOR and S6 in CD4$^+$ T cells cultured alone or stimulated with anti-CD3/CD28 beads in the absence or presence of activated B cells for 48 hours. Activated B cells were pretreated with DMSO (solvent control) or LDH inhibitor. Data are representative of two independent experiments with n=2 individual samples. Statistical analysis by repeated measures one-way ANOVA (B, C, H, I) or ordinary one-way ANOVA (D, E, F, G) with Bonferroni's correction for multiple comparisons. ANOVA, analysis of variance; CFSE, carboxyfluorescein succinimidyl ester; FDR, false discovery rate; LDH, lactate dehydrogenase; MFI, median fluorescent intensity; mTOR, mammalian target of rapamycin; NS, not significant; p-mTOR, phospho-mTOR. *p≤0.05, **p≤0.01, ***p≤0.001.

PD-L1, and PD-1 compared with other B cell clusters (p≤0.001), suggesting its immunosuppressive function and the possible contribution of this B cell cluster to ICB therapy failure (figure 5D). On the other hand, cluster #5, characterized by higher expression of CD95, was upregulated in responders compared with non-responders (figure 5C,D). Interestingly, B cells stimulated with CD40L and IL-4, which are reported to function as antigen-presenting cells,[29] also had higher expression of CD95 (figure 5B). Thus, CD95 may serve as a marker for B cells with effector function.

Finally, we compared the expression of genes related to B cell activation, glycolysis, and OXPHOS in TABs in head and neck squamous cell cancer, lung cancer, and melanoma with those in B cells of normal bone marrow (control). ScRNA-seq data from a public database demonstrated increased expression of genes related to B cell activation, including *ENTPD1* (CD39), *CD80*, *CD274*

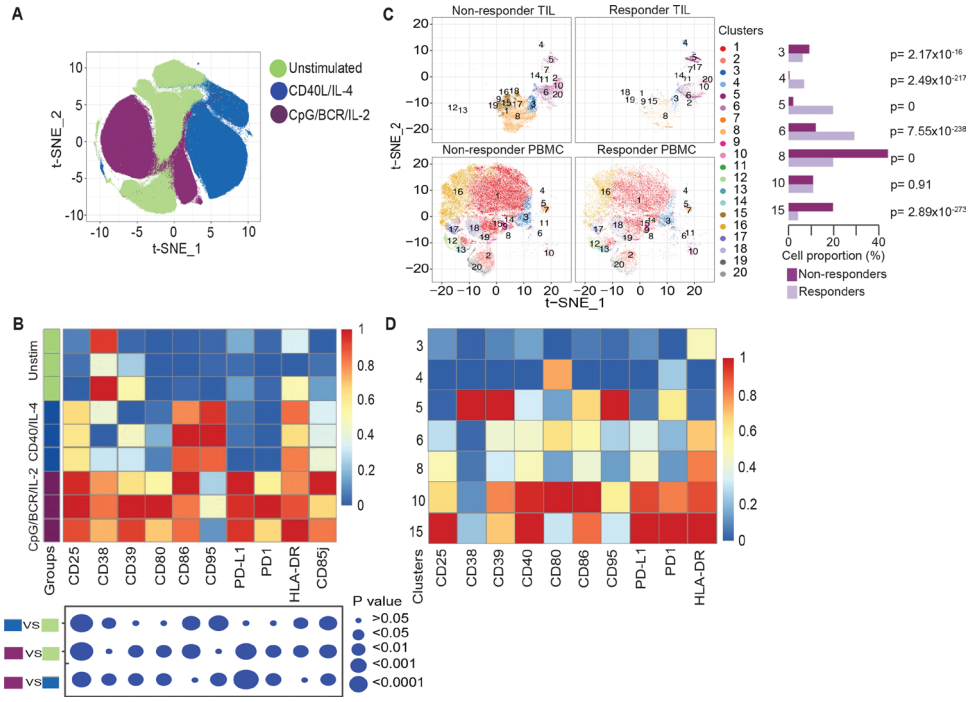

Figure 5 B cells with immunosuppressive phenotype can be identified in human melanoma tissues and are associated with poor response to immune checkpoint blockade therapy. viSNE plot (A) and comparative mass cytometry heatmap (B) showing phenotype of unstimulated B cells, B cells stimulated with CD40 ligand and IL-4, and B cells stimulated with CpG, anti-IgG/IgM, and IL-2. Each row of heatmap represents B cells from a different donor (n=3) and each column represents the normalized expression of a certain marker for each annotation. Expression levels were normalized over columns. Color scale ranges from blue (low expression) to red (high expression). The FDR-adjusted p values for each gene are shown under the heat map.(C, D) viSNE plot faceted by responder (n=6) versus non-responder (n=6) and PBMC versus tumor infiltrating lymphocytes (TIL) (C) and comparative mass cytometry heatmap (D) showing the expression of peripheral blood and tumor-associated B cells from responders and non-responders among patients with melanoma who received immune checkpoint blockade therapy. The viSNE map generated from FlowSOM analysis (C) shows the 20 clusters of B cells in peripheral blood and tumors. The clusters represented in the bar graph (C) were identified in the TIL and show the percentage of non-responder cells and responder cells at each cluster. Fisher's exact test was performed to compare the proportion of cells . The p value is shown for each comparison. In the heatmap (D) each row of heatmap represents B cells of different TIL clusters and each column represents the normalized expression of a certain marker for each annotation. Expression levels were normalized over columns to a range of 0 (blue) to 1 (red). FDR, false discovery rate; IL, interleukin; PBMC, peripheral blood mononuclear cells; t-SNE, t-distributed stochastic neighbor-embedding.

(PD-L1), and *PDCD1* (PD-1), in TABs compared with normal bone marrow B cells (figure 6A, online supplemental figure S11A), suggesting that TABs are activated and have immunosuppressive function. Glycolysis-related and OXPHOS-related genes were also upregulated in TABs compared with normal bone marrow B cells (figure 6B,C, online supplemental figure S11B,C). A similar trend was observed when the scRNA-seq data for B cells from lung cancer were compared with those from normal lung tissues, suggesting that these differences are not a reflection of tissue differences in oxygen availability (online supplemental figure S12). Collectively, these results support our view that TABs contribute to the progression of tumors and treatment failure by inhibiting antitumor T-cell response through their high metabolic activity.

DISCUSSION

Several lines of studies have shown that metabolic activity of cells have immunomodulatory effects. A variety of tumors and tumor associated myeloid-derived suppressor cells degrade tryptophan to kynurenine by indoleamine 2,3-dioxygenase, which cause depletion of tryptophan, an important amino acid required for T-cell activation, and accumulation of kynurenine, an immunosuppressive metabolite.[35] In addition to amino acid metabolism, recent studies have revealed immunomodulatory effects of glucose metabolism. Highly glycolytic tumors impair antitumor immunity through glucose deprivation and/or lactic acid production.[12 13] Activated T cells deprive dendritic cells of glucose to enhance capacity of dendritic cells to induce T-cell response.[36] Adding to these previous studies, here we demonstrated for the first time that activated B cells inhibit T-cell function through their metabolic activity. Of note, this inhibition was achieved not only through their high glycolytic activity, but also through their high OXPHOS activity. Activated B cells induced

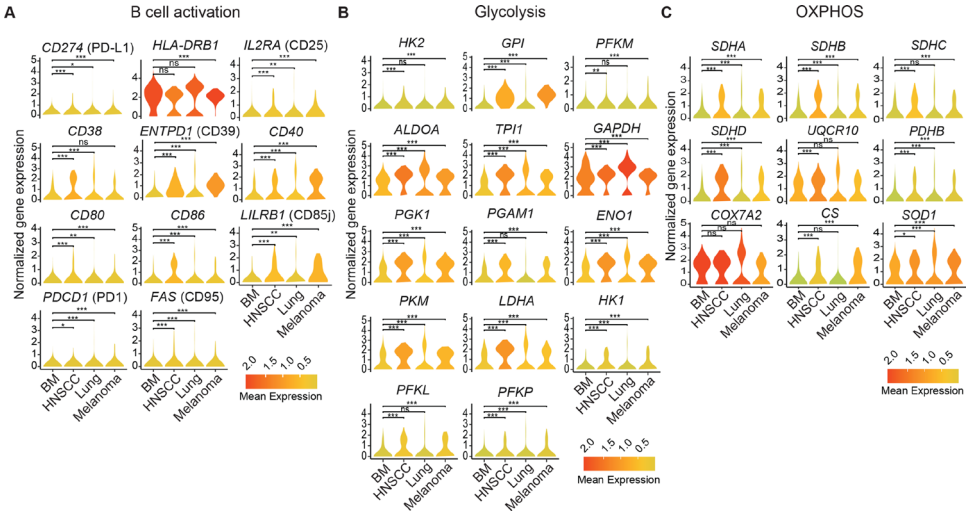

Figure 6 Tumor-associated B cells display an activated phenotype and have high glycolytic and OXPHOS activity. Violin plots showing the messenger RNA expression levels for individual B cell activation (A), glycolysis (B), and oxidative phosphorylation (OXPHOS) (C) genes in tumor-associated B cells from head and neck squamous cell carcinoma (HNSCC), lung cancer, melanoma and B cells from bone marrow (BM) using single-cell RNA sequencing. The color represents the average expression level for a given gene in the cluster normalized using Seurat V.3.0 NormalizeData function. Statistical analysis by Wilcoxon rank-sum. P values were adjusted by the Benjamini-Hochberg method. ns, not significant; *p≤0.05, **p≤0.01, ***p≤0.001.

hypoxia in T cells by consuming oxygen via OXPHOS, and thereby inhibited mTOR signaling pathway and effector function of T cells. Collectively, these findings indicate that the immunomodulatory effects of the metabolic machinery of cells are not specific to certain cell types nor are they specific to certain metabolic pathways. Rather, immunomodulation by the metabolic machinery of cells appears to be a widely occurring phenomenon.

Although the inhibitory effects of lactic acid on T-cell function are well established, the mechanism remains unclear. One study reported that lactic acid suppressed anti-CD3-induced phosphorylation of p38 and JNK without affecting that of ERK and AKT.[37] Another study showed that lactic acid lowered intracellular pH and impaired PMA/Iono-induced-upregulation of nuclear factor of activated T-cells (NFAT) while modestly inhibiting phosphorylation of p38 and AKT.[13] Here, we showed that lactic acid suppressed anti-CD3/CD28-induced phosphorylation of the mTOR pathway components. These variable results may be explained by differences in stimulation methods and studied pathways. More comprehensive studies are necessary to elucidate the mechanisms of T-cell suppression by lactic acid. This is particularly important as understanding the mechanism by which lactic acid suppresses T-cell function may lead to development of novel strategy to overcome T-cell inhibition by lactic acid produced by tumors.

We demonstrated that the metabolic activity of activated B cells was further enhanced by stimulated $CD4^+$ T cells. In an attempt to identify the molecules responsible for this observation, CD40, IL-2Rα, and IL-21 receptor genes in activated B cells were knocked out using CRISPR/Cas9 system because these proteins have been reported to be involved in the B cell activation by $CD4^+$ T cells.[38–40] However, knockout of these genes did not prevent enhancement of OCR in activated B cells by $CD4^+$ T cells (data not shown). It is possible that the activating signals from a knocked-out protein might have been compensated for by the activating signals from the other proteins. Alternatively, other molecules might have been responsible for $CD4^+$ T cell-mediated enhancement of metabolic activity in activated B cells. T cells receive activating signals from the interaction of their co-stimulatory molecules with cognate ligands on antigen presenting cells, including B cells. However, some studies have reported that activating signals are bidirectional.[41] Thus, it is possible that $CD4^+$ T cell-induced enhancement in the metabolism of activated B cells was caused by positive signals from co-stimulatory molecules such as inducible T-cell costimulator (ICOS) ligand. Identification of molecules responsible for T cell-facilitated enhancement in metabolism of activated B cells may provide therapeutic strategies to inhibit unwanted T-cell suppression by activated B cells.

Various subsets of human peripheral blood B cells which can suppress T-cell function without ex vivo manipulation have been identified. These include CD24hiCD38hi B cells, $TIM1^+$ B cells, and $CD73^-CD25^+CD71^+$ B cells, and represent a small population of peripheral blood B cells.[42] On the other hand, the present study demonstrated that total peripheral blood B cells from healthy donors acquire immunosuppressive properties on activation, in line with previous studies.[3–6] Importantly, T cell-induced enhancement in the metabolic activity of activated B cells contributed to the suppression of T cells by activated B cells, supporting a regulatory feedback role for activated B cells. This view is further supported by the observation that peripheral blood B cells from patients with autoimmune disease were defective in acquiring immunosuppressive properties after stimulation.[4 5] Moreover, B cells

with similar phenotype and function as TABs (which inhibit antitumor T-cell response) can be induced by stimulating peripheral blood B cells with IL-21 with or without B cell receptor (BCR) agonist, or TLR agonists.[7 8] Collectively, these observations suggest that the regulatory function of B cells is not confined to a small subset of B cells and that B cells possess functional plasticity that is determined by environmental stimuli.

Numerous studies have shown that B cells are present in the microenvironment of various types of human cancers. Moreover, TABs were shown to promote the progression of tumors by directly stimulating tumor cell proliferation, promoting angiogenesis, and inhibiting antitumor immune response by directly suppressing effector T-cells and/or inducing Treg.[8 34 43] Here, we showed that activated B cells, which suppressed T-cell function through their high metabolic activity, were characterized by the high expression of B cell activation markers including CD39, CD80, PD-L1, and PD-1, and that B cells with similar phenotype were increased in tumor tissues of patients who failed to respond to ICB therapy (figure 5). In addition, TABs were shown to have higher expression of OXPHOS and/or glycolysis-related genes further supporting their high metabolic activity (figure 6). These results suggest a novel mechanism of TAB-mediated tumor promotion whereby TABs inhibit antitumor T-cell response by metabolically restricting T cells through their high metabolic activity.

However, other studies have also reported important antitumor properties for TABs.[43 44] These conflicting reports indicate the dual functions of B cells in the tumor microenvironment. In this regard, localization of B cells within tumor tissues may also play an important role. Considering that tertiary lymphoid structures (TLS) containing B cells were associated with a better response to ICB therapy in melanoma,[17] immunosuppressive activated B cells identified in our study may be located outside TLS. Comparing the phenotype of B cells within and outside TLS may provide additional insights into the prognostic relevance of TABs. In the present study, B cells stimulated with CpG, anti-IgG/IgM, and IL-2, but not those stimulated with CD40L and IL-4, acquired suppressive properties. This finding is partly in line with a previous study which showed that IL-4 stimulation abolished TLR signaling-mediated induction of protumor B cells.[8] Other studies reported that melanoma-derived fibroblast growth factor-2 (FGF-2) and glioma cell-derived placental growth factor induce conversion of normal B cells into protumor B cells.[43] Despite these findings, the mechanisms by which B cells are induced to become protumor or antitumor in the tumor microenvironment are still largely unknown. Better understanding of these mechanisms may lead to the development of novel treatments that convert protumor B cells into antitumor B cells, and thereby inhibit tumor progression. While our study revealed an association between activated B cells with an immunosuppressive phenotype and ICB therapy failure (figure 5), further research is needed to better understand the interaction of B cells and T cells within the tumor microenvironment.

In summary, we have revealed for the first time the immunomodulatory effects of the metabolic activity of activated B cells, which are mediated not only by glycolysis, but also by OXPHOS, and their possible role in suppressing antitumor T-cell responses. These findings add novel insights into immunometabolism and have important implications for cancer immunotherapy.

Author affiliations
[1]Department of Stem Cell Transplantation and Cellular Therapy, The University of Texas MD Anderson Cancer Center, Houston, Texas, USA
[2]Department of Hematology, National Hospital Organization Nagoya Medical Center, Nagoya, Japan
[3]Department of Bioinformatics and Computational Biology, The University of Texas MD Anderson Cancer Center, Houston, Texas, USA
[4]Department of Leukemia, The University of Texas MD Anderson Cancer Center, Houston, Texas, USA
[5]Departments of Stem Cell Transplantation and Hemotherapy/Cellular Therapy, Hospital Israelita Albert Einstein, Sao Paulo, Brazil
[6]Human Genome and Stem Cell Research Center, Department of Genetics and Evolutionary Biology, Biosciences Institute, University of São Paulo (USP), Sao Paulo, Brazil
[7]Department of Lymphoma and Myeloma, The University of Texas MD Anderson Cancer Center, Houston, Texas, USA
[8]Department of Genomic Medicine, The University of Texas MD Anderson Cancer Center, Houston, TX, USA
[9]Department of Surgical Oncology, The University of Texas MD Anderson Cancer Center, Houston, TX, USA

Contributors NI, RB, and KR conducted conceptualization of the study, experimental design, interpreted and analyzed data. YH, FW, and RB performed single-cell RNA sequencing and mass cytometry experiments and analysis. NB, and AKNC performed Seahorse assays. PPB performed Imageflow experiments. FW, JL, NU, EE, MD, MM, LNK, MS, LL, FLWIL, HS, and YL assisted with experiments. MK, MG, JW, KC and EJS provided advice with experiments. NI, LM-F, TJL, JSM, and KR wrote, reviewed and edited the manuscript. KR is responsible for the overall content as guarantor.

Funding NI received financial support from the Japan Society for the Promotion of Science (JSPS) as JSPS Overseas Research Fellow. This work was supported in part by the generous philanthropic contributions to The University of Texas MD Anderson Cancer Center Moon Shots Program and The Sally Cooper Murray endowment; by Grants (1 R01 CA211044-01, 5 P01CA148600-03, U01CA247760, and R01CA231364) from the National Institutes of Health (NIH), CPRIT (RP180466), the Leukemia Specialized Program of Research Excellence (SPORE) Grants (P50CA100632, FP00015401), and the Grant (P30 CA016672) from the NIH to the MD Anderson Cancer Center Flow Cytometry and Cellular Imaging Core Facility that assisted with the mass cytometry studies.

Competing interests KR, RB, PPB, MD, LNK, EJS and The University of Texas MD Anderson Cancer Center have an institutional financial conflict of interest with Takeda Pharmaceutical. KR, RB, LNK, EJS, and The University of Texas MD Anderson Cancer Center have an institutional financial conflict of interest with Affimed GmbH. KR participates on the Scientific Advisory Board for GemoAb, Avenge Bio, Virogin Biotech, GSK, Caribou Biosciences, Navan Technologies and Bayer. The remaining authors declare no competing financial interests.

Patient consent for publication Not applicable.

Ethics approval This study involves human participants. All patients gave informed consent to participate per The University of Texas MD Anderson Cancer Center Institutional Review Board (IRB)-approved protocols (2015-0041, 2012-0846). All studies were performed in accordance with the Declaration of Helsinki. Participants gave informed consent to participate in the study before taking part.

Provenance and peer review Not commissioned; externally peer reviewed.

Data availability statement Data are available upon reasonable request.

ORCID iDs
Ye Li http://orcid.org/0000-0001-7727-0875
Katayoun Rezvani http://orcid.org/0000-0002-9599-2246

REFERENCES

1 Khoder A, Sarvaria A, Alsuliman A, *et al*. Regulatory B cells are enriched within the IgM memory and transitional subsets in healthy donors but are deficient in chronic GVHD. *Blood* 2014;124:2034–45.
2 Blair PA, Noreña LY, Flores-Borja F, *et al*. CD19(+)CD24(hi)CD38(hi) B cells exhibit regulatory capacity in healthy individuals but are functionally impaired in systemic Lupus Erythematosus patients. *Immunity* 2010;32:129–40.
3 Nouël A, Pochard P, Simon Q, *et al*. B-Cells induce regulatory T cells through TGF-β/IDO production in a CTLA-4 dependent manner. *J Autoimmun* 2015;59:53–60.
4 Bankó Z, Pozsgay J, Szili D, *et al*. Induction and differentiation of IL-10-producing regulatory B cells from healthy blood donors and rheumatoid arthritis patients. *J Immunol* 2017;198:1512–20.
5 Gao N, Dresel J, Eckstein V, *et al*. Impaired suppressive capacity of activation-induced regulatory B cells in systemic lupus erythematosus. *Arthritis Rheumatol* 2014;66:2849–61.
6 Tretter T, Venigalla RKC, Eckstein V, *et al*. Induction of CD4+ T-cell anergy and apoptosis by activated human B cells. *Blood* 2008;112:4555–64.
7 Lindner S, Dahlke K, Sontheimer K, *et al*. Interleukin 21-induced granzyme B-expressing B cells infiltrate tumors and regulate T cells. *Cancer Res* 2013;73:2468–79.
8 Xiao X, Lao X-M, Chen M-M, *et al*. PD-1hi identifies a novel regulatory B-cell population in human hepatoma that promotes disease progression. *Cancer Discov* 2016;6:546–59.
9 Mauri C, Gray D, Mushtaq N, *et al*. Prevention of arthritis by interleukin 10-producing B cells. *J Exp Med* 2003;197:489–501.
10 Korniotis S, Gras C, Letscher H, *et al*. Treatment of ongoing autoimmune encephalomyelitis with activated B-cell progenitors maturing into regulatory B cells. *Nat Commun* 2016;7:12134.
11 Akkaya M, Traba J, Roesler AS, *et al*. Second signals rescue B cells from activation-induced mitochondrial dysfunction and death. *Nat Immunol* 2018;19:871–84.
12 Chang C-H, Qiu J, O'Sullivan D, *et al*. Metabolic competition in the tumor microenvironment is a driver of cancer progression. *Cell* 2015;162:1229–41.
13 Brand A, Singer K, Koehl GE, *et al*. LDHA-Associated lactic acid production blunts tumor immunosurveillance by T and NK cells. *Cell Metab* 2016;24:657–71.
14 Uhl FM, Chen S, O'Sullivan D, *et al*. Metabolic reprogramming of donor T cells enhances graft-versus-leukemia effects in mice and humans. *Sci Transl Med* 2020;12:eabb8969.
15 Waickman AT, Powell JD. Mammalian target of rapamycin integrates diverse inputs to guide the outcome of antigen recognition in T cells. *J Immunol* 2012;188:4721–9.
16 Tian C, Kron GK, Dischert KM, *et al*. Low expression of the interleukin (IL)-4 receptor alpha chain and reduced signalling via the IL-4 receptor complex in human neonatal B cells. *Immunology* 2006;119:54–62.
17 Helmink BA, Reddy SM, Gao J, *et al*. B cells and tertiary lymphoid structures promote immunotherapy response. *Nature* 2020;577:549–55.
18 Piao W, Tsuda S, Tanaka Y, *et al*. Development of azo-based fluorescent probes to detect different levels of hypoxia. *Angew Chem Int Ed Engl* 2013;52:13028–32.
19 LaGory EL, Giaccia AJ. The ever-expanding role of HIF in tumour and stromal biology. *Nat Cell Biol* 2016;18:356–65.
20 Nakamura H, Makino Y, Okamoto K, *et al*. Tcr engagement increases hypoxia-inducible factor-1 alpha protein synthesis via rapamycin-sensitive pathway under hypoxic conditions in human peripheral T cells. *J Immunol* 2005;174:7592–9.
21 Volchenkov R, Nygaard V, Sener Z, *et al*. Th17 polarization under hypoxia results in increased IL-10 production in a Pathogen-Independent manner. *Front Immunol* 2017;8:698.
22 Molina JR, Sun Y, Protopopova M, *et al*. An inhibitor of oxidative phosphorylation exploits cancer vulnerability. *Nat Med* 2018;24:1036–46.
23 Price MJ, Patterson DG, Scharer CD, *et al*. Progressive upregulation of oxidative metabolism facilitates Plasmablast differentiation to a T-independent antigen. *Cell Rep* 2018;23:3152–9.
24 Campbell EL, Bruyninckx WJ, Kelly CJ, *et al*. Transmigrating neutrophils shape the mucosal microenvironment through localized oxygen depletion to influence resolution of inflammation. *Immunity* 2014;40:66–77.
25 Khan AR, Hams E, Floudas A, *et al*. PD-L1hi B cells are critical regulators of humoral immunity. *Nat Commun* 2015;6:5997.
26 Busse D, de la Rosa M, Hobiger K, *et al*. Competing feedback loops shape IL-2 signaling between helper and regulatory T lymphocytes in cellular microenvironments. *Proc Natl Acad Sci U S A* 2010;107:3058–63.
27 Baba T, Otake H, Sato T, *et al*. Glycolytic genes are targets of the nuclear receptor Ad4BP/SF-1. *Nat Commun* 2014;5:3634.
28 Blagih J, Coulombe F, Vincent EE, *et al*. The energy sensor AMPK regulates T cell metabolic adaptation and effector responses in vivo. *Immunity* 2015;42:41–54.
29 von Bergwelt-Baildon MS, Vonderheide RH, Maecker B, *et al*. Human primary and memory cytotoxic T lymphocyte responses are efficiently induced by means of CD40-activated B cells as antigen-presenting cells: potential for clinical application. *Blood* 2002;99:3319–25.
30 Carpenter EL, Mick R, Rüter J, *et al*. Activation of human B cells by the agonist CD40 antibody CP-870,893 and augmentation with simultaneous Toll-like receptor 9 stimulation. *J Transl Med* 2009;7:93.
31 Ambegaonkar AA, Nagata S, Pierce SK, *et al*. The Differentiation *in vitro* of Human Tonsil B Cells With the Phenotypic and Functional Characteristics of T-bet+ Atypical Memory B Cells in Malaria. *Front Immunol* 2019;10:852.
32 Thibult M-L, Mamessier E, Gertner-Dardenne J, *et al*. Pd-1 is a novel regulator of human B-cell activation. *Int Immunol* 2013;25:129–37.
33 Saze Z, Schuler PJ, Hong C-S, *et al*. Adenosine production by human B cells and B cell-mediated suppression of activated T cells. *Blood* 2013;122:9–18.
34 Shang J, Zha H, Sun Y. Phenotypes, functions, and clinical relevance of regulatory B cells in cancer. *Front Immunol* 2020;11:582657.
35 Thommen DS, Schumacher TN. T cell dysfunction in cancer. *Cancer Cell* 2018;33:547–62.
36 Lawless SJ, Kedia-Mehta N, Walls JF, *et al*. Glucose represses dendritic cell-induced T cell responses. *Nat Commun* 2017;8:15620.
37 Mendler AN, Hu B, Prinz PU, *et al*. Tumor lactic acidosis suppresses CTL function by inhibition of p38 and JNK/c-Jun activation. *Int J Cancer* 2012;131:633–40.
38 Bishop GA, Hostager BS. B lymphocyte activation by contact-mediated interactions with T lymphocytes. *Curr Opin Immunol* 2001;13:278–85.
39 Mingari MC, Gerosa F, Carra G, *et al*. Human interleukin-2 promotes proliferation of activated B cells via surface receptors similar to those of activated T cells. *Nature* 1984;312:641–3.
40 Kuchen S, Robbins R, Sims GP, *et al*. Essential role of IL-21 in B cell activation, expansion, and plasma cell generation during CD4+ T cell-B cell collaboration. *J Immunol* 2007;179:5886–96.
41 Mak TW, Shahinian A, Yoshinaga SK, *et al*. Costimulation through the inducible costimulator ligand is essential for both T helper and B cell functions in T cell-dependent B cell responses. *Nat Immunol* 2003;4:765–72.
42 Mauri C, Menon M. Human regulatory B cells in health and disease: therapeutic potential. *J Clin Invest* 2017;127:772–9.
43 Largeot A, Pagano G, Gonder S, *et al*. The B-side of cancer immunity: the underrated tune. *Cells* 2019;8:449.
44 Wouters MCA, Nelson BH. Prognostic significance of tumor-infiltrating B cells and plasma cells in human cancer. *Clin Cancer Res* 2018;24:6125–35.